Journal of Power Sources 195 (2010) 5370–5373

Contents lists available at ScienceDirect

Journal of Power Sources

journal homepage: www.elsevier.com/locate/jpowsour

Short communication

Effect of ethanol-assisted electrode fabrication on the performance of silicon anodes

Sigita Urbonaite*, Ida Baglien, David Ensling, Kristina Edström

Department of Materials Chemistry, The Ångström Laboratory, Uppsala University, Box 538, SE-75121 Uppsala, Sweden

ARTICLE INFO

Article history:
Received 22 December 2009
Received in revised form 9 March 2010
Accepted 12 March 2010
Available online 19 March 2010

Keywords:
Li-ion batteries
Si-based anodes
XPS analysis
Nano-silicon
Ethanol treatment

ABSTRACT

The performance of high-silicon-content anodes was tested as a function of silicon particle-size (44 μm, 1.8 μm and 70–100 nm), surface pre-treatment and solvent chosen for anode preparation. Two simple procedures, leading to significant improvements in electrode performance are reported. First, pre-treatment of nano-Si in ethanol which unexpectedly yields functionalised surfaces improving cycling stability. Second, the use of a 30:70 solution of ethanol and water to dissolve the CMC-binder for the electrode preparation boosts specific battery capacity. Ethanol pre-treatment of nano-Si also resulted in improved adhesion of the electrode to the current collector as well as in de-agglomeration of nano-Si powder. All these treatments improved capacity stability during cycling. Changes in surface chemistry of nano-Si before and after ethanol treatment have been analysed by XPS. A stable capacity of about 1630 mAh g^{-1} was obtained after 25 cycles for an electrode containing 80% silicon using ethanol during electrode coating preparation.

1. Introduction

Lithium-ion batteries have a number of advantages relative to other types of secondary batteries, including higher energy density, higher operating voltages and lower self-discharge. However further improvements of Li-ion batteries are needed due to growing performance demands of portable technologies. As shown in the review by Kasavajjula et al. [1], the total capacity of Li-ion cells depends on the capacities of both anode and cathode. The total capacity of the cell increases until the anode capacity reaches ~1200 mAh g^{-1} with current limit in cathode capacities being 140–200 mAh g^{-1}. This suggests that carbon-based anodes need to be replaced with anodes able to offer capacities of at least 1200 mAh g^{-1} [2]. One of the most promising anode materials to offer such high capacity is silicon.

Silicon can alloy with lithium, taking in up to 4.4 Li atoms per Si atom, resulting in a specific capacity of up to 4200 mAh g^{-1}. Besides providing high capacity, Si is light and, as one of the most abundant elements on Earth, it is an ideal candidate for the next generations of anodes. A crucial problem with a view to Si-based anode implementation is its volume expansion of up to 400% at full lithiation [3]. There are several ways to overcome this problem, such as decreasing particle-size, using composites with active and inactive matrixes as well use of different binders. So far the highest capacities are reported for Si nanowires [4], and Si thin-films [5]. Anode fabrication by traditional thick-film methods typically involves the use of low-Si content, carbon-coated silicon or results in lower specific capacity, high rate of capacity fading, etc. [1,6–9].

The way of easy implementation of new types of anodes is to have simple, inexpensive methods for Si-anode production, which will not require significant technological changes. In the present study, we tested the performance of anodes with high (~80%) amount of Si depending on particle-size, pre-treatment by ultrasonication in ethanol, and on solvent composition during anode preparation stage using traditional thick-film electrode coating method.

2. Experimental

2.1. Electrode preparation

Two types of silicon powders were used to produce electrodes: 80% of bulk-Si (particle-size 44 μm, Aldrich) or nano-Si (particle-size 70–100 nm, Sigma–Aldrich) were mixed with 12% carbon black (Super P, MMM) and 8% of sodium carboxymethyl cellulose (CMC; M_w = 700,000, Sigma–Aldrich) as a binder by milling either in a SPEX/CertiPrep high-energy ball mill for 30 min or in a planetary mill for 60 min. Electrodes were made using both silicon types: as received or ethanol-treated for 3 h in an ultrasonic bath. Furthermore, two types of solvents for slurry preparation were used: water and ethanol–water (EtOH:$H_2O \approx$ 30:70) solution. The resulting slurry was casted on 0.02 mm thick copper foil and dried at 90 °C

* Corresponding author. Tel.: +46 18 4713776; fax: +46 18 513548.
E-mail address: sigita.urbonaite@mkem.uu.se (S. Urbonaite).

0378-7753/$ – see front matter © 2010 Elsevier B.V. All rights reserved.
doi:10.1016/j.jpowsour.2010.03.042

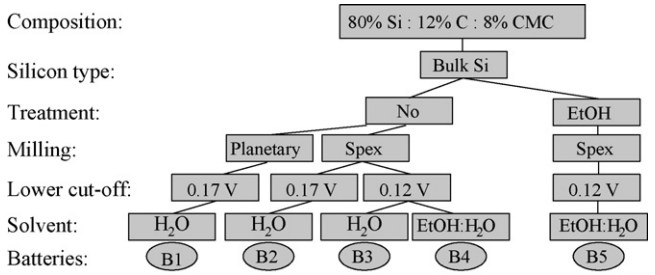

Fig. 1. Electrode preparation and cycling characteristics applied to each bulk-Si-based battery.

overnight. Circular electrodes (area of 3.14 cm^2) were stamped out from electrode coatings and dried overnight at 120 °C in a vacuum oven inside a glove box (<3 ppm O_2, <1 ppm H_2O). Pouch type cells were assembled by stacking the electrode, a glass-fibre separator soaked with electrolyte (1 M $LiPF_6$ dissolved in ethylene carbonate/dimethyl carbonate with ratio EC:DEC 2:1) and a lithium foil. The assembly was then vacuum sealed into a polymer-coated aluminium pouch with attached nickel tabs as current collectors.

2.2. Electrochemical testing

The electrochemical testing was done on a Digatron BTS-600. Four pre-cycles were performed prior to standard galvanostatic cycling between 0.12 or 0.17 and 0.9 V. In the pre-cycling, the electrodes were discharged to 500, 1000, 1500 and 2000 mAh g^{-1} and charged to 0.9 V, respectively. The current during all electrochemical testing was 150 mA g^{-1}. The starting recipe and pre-cycling procedure were adopted from Li et al. [10]. More detailed information about the different preparation and cycling protocols for all batteries tested is given in Figs. 1 and 2. Batteries N1 and N2, as well as N3 and N4 are from separate slurry preparation batches, assembled and electrochemically cycled under identical conditions for reproducibility purposes.

2.3. Morphology and surface analysis

The morphologies of all electrodes were examined using scanning electron microscope (SEM) operated at 10–15 kV. XPS measurements were performed on a PHI 5500 system equipped with a monochromatic Al Kα X-ray source (1486.6 eV). The spectrometer energy scale was calibrated using $Cu2p_{3/2}$ (932.7 eV),

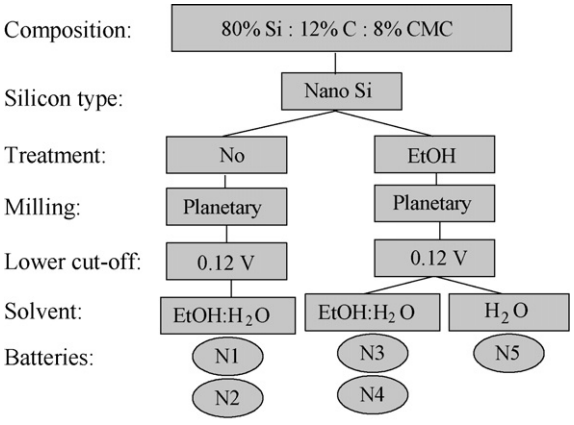

Fig. 2. Electrode preparation and cycling characteristics applied to each nano-Si-based battery.

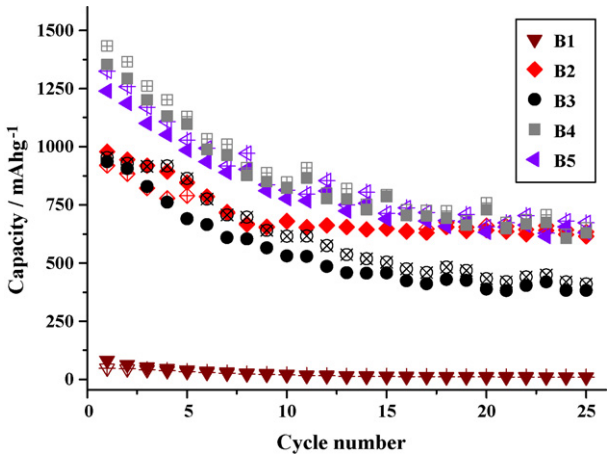

Fig. 3. Charge and discharge capacities of bulk-Si-based electrodes vs. cycle number. Filled symbols are for charge and open symbols for discharge capacities. Pre-cycling is excluded.

$Ag3d_{5/2}$ (386.2 eV) and $Au4f_{7/2}$ (84.0 eV) emissions of 3 keV sputter-cleaned metal foils. The silicon powders were pressed onto Al-foils for the measurement in order to provide a conductive substrate. The ethanol-treated and non-treated Si powders were handled in air. The spectral background was removed using a Tougaard-type correction function. For peak fitting Voigt-type function has been applied.

3. Results and discussion

3.1. Electrode performance and characterisation

The performance of all 10 batteries was tested and the influence of three parameters (particle-size, solvent used in production of electrode coatings, and ethanol pre-treatment of starting silicon powders) was investigated.

Three different particle sizes were compared: 44 μm bulk-Si, 1–8 μm bulk-Si (size reduction is a result of hard milling in SPEX/CertiPrep high-energy ball mill) and 70–100 nm nano-Si. The electrode containing the largest silicon particles (B1) had no measurable capacity, see Fig. 3.

The reason for this can be that the surface of anode's B1 film is very uneven, with large Si particles visible in the SEM micrograph (see Fig. 5), which might cause a bad contact between the electrode components. The electrodes with the smallest particle-size (N1 and N2) had very high initial capacity, but after 25 cycles it was comparable to that of anodes with intermediate silicon particle-size (B2–B5).

The intermediate particle-size electrodes (in Fig. 5, electrode B5 is given as an example) have smooth, even surfaces with no cracks, resulting in significantly improved capacity. The nano-Si-based electrode surfaces are also smooth, but cracked. Electrode N1 has larger cracks and poorer adhesion to the copper foil than N3, which has also fewer agglomerations; the latter was achieved by treating nano-Si powder in ethanol. The treatment does not result in higher initial capacity, but clearly is one of the factors leading to a high and stable capacity over all 25 cycles, see Figs. 4 and 5.

When the EtOH:H_2O solution was used as a solvent in electrode preparation, higher capacities were achieved compared to the batteries where only water is used. In case of bulk-Si-based anodes, using EtOH: H_2O mixture resulted in an initial capacity increase of about 500 mAh g^{-1}, but after 25 cycles there was no significant difference between batteries B2 (H_2O as a solvent) and B4 (EtOH:H_2O as a solvent), see Fig. 3. Nano-Si-based electrodes (N1 and N2),

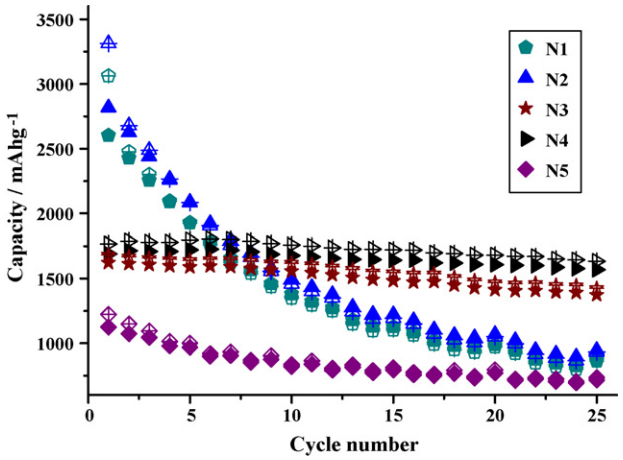

Fig. 4. Charge and discharge capacities of nano-Si-based electrodes vs. cycle number. Filled symbols are for charge and open symbols for discharge capacities. Pre-cycling is excluded.

untreated in ethanol but using EtOH:H_2O solution as a solvent, exhibits initial capacity above 2000 mAh g^{-1}, but very high capacity fading-rate; the capacity after 25 cycles is 875 mAh g^{-1}, which is only about 250 mAh g^{-1} higher than that of bulk-Si, see Figs. 3 and 4.

Four batteries were made using ethanol pre-treated silicon powders. Pre-treatment with ethanol of the bulk-Si (B5) and using EtOH:H_2O solution as solvent did not improve the capacity of the batteries. However, ethanol pre-treatment resulted in a significant effect on the performance of nano-Si-based batteries (N3 and N4). The capacity of the first cycles was high but much lower than non-treated nano-Si-based batteries (N1 and N2), albeit with very low capacity fade. Final capacities after 25 cycles were 1630 mAh g^{-1} (N3) and 1420 mAh g^{-1} (N4). The last battery (B10) based on pre-treated nano-Si, but using H_2O as a solvent for electrode preparation, does not have higher capacity than prepared from bulk-Si, which indicates the importance of ethanol presence during electrode film preparation.

3.2. Ethanol pre-treatment effect on the surface of nano-Si

In order to investigate changes induced by ethanol pre-treatment on to the surface of nano-Si and find an explanation to the improvement of battery performance, both, ethanol-treated and untreated, silicon powders have been investigated by XPS. The core-level spectra of the O1s, Si2p and C1s emissions are shown in Fig. 6. The Si2p emission (DS Si2p3/2–Si2p1/2: 0.61 eV) reveals contributions from Si/SiH bonds at lower binding energies around EB (Si/SiH) = 97.2 eV, and from higher oxidized species – in particular SiO_x suboxides and SiO_2 – at higher energies. The binding energies of the dominating SiO_x peak are 99.8 eV and 99.0 eV for the untreated and ethanol-treated silicon, respectively. The shift in binding energy for about 0.8 eV can be attributed to a change in conductivity of the material as discussed by Bolotov et al. [11]. The X-ray induced charging of the sample shifts the SiO_x peak position of the untreated sample to higher binding energies. This interpretation is supported by the observation of a significantly larger spectral line width for the untreated silicon. For all other peaks in the O1s, Si2p and C1s emission lines, spectral broadening, but only a shift of ~0.2 eV is observed.

Furthermore, the relative intensity of the Si2p peak decreases for the ethanol-treated material, indicating the formation of an additional surface layer (see Fig. 6). This is also apparent in the C1s emission. The surface layer contains aliphatic carbon (EB = 284.5 eV) and oxidized carbon compounds (C–O, C–OH; EB = 286.5 eV) as well as small amounts of carbonates (EB = 288.5 eV). The relative intensity of the C1s peak is significantly higher for the ethanol-treated sample. In the case of the ethanol-treated sample, the O1s emission shows contributions of SiO_x and SiO_2 species at EB = 532.3 eV and EB = 533.6 eV, respectively. The peak at EB = 530.0 eV cannot be identified conclusively, but originates probably from carbon surface species. Finally, XPS results reveal an increased amount of carbon species and a relative increase of the Si/SiH features in the Si2p emission.

In Section 3.1 it was established that ultrasonication of nano-Si in ethanol significantly improves cycling stability. This implies changes in nano-Si surface chemistry and this was confirmed by XPS studies. There are number of reactions which may occur

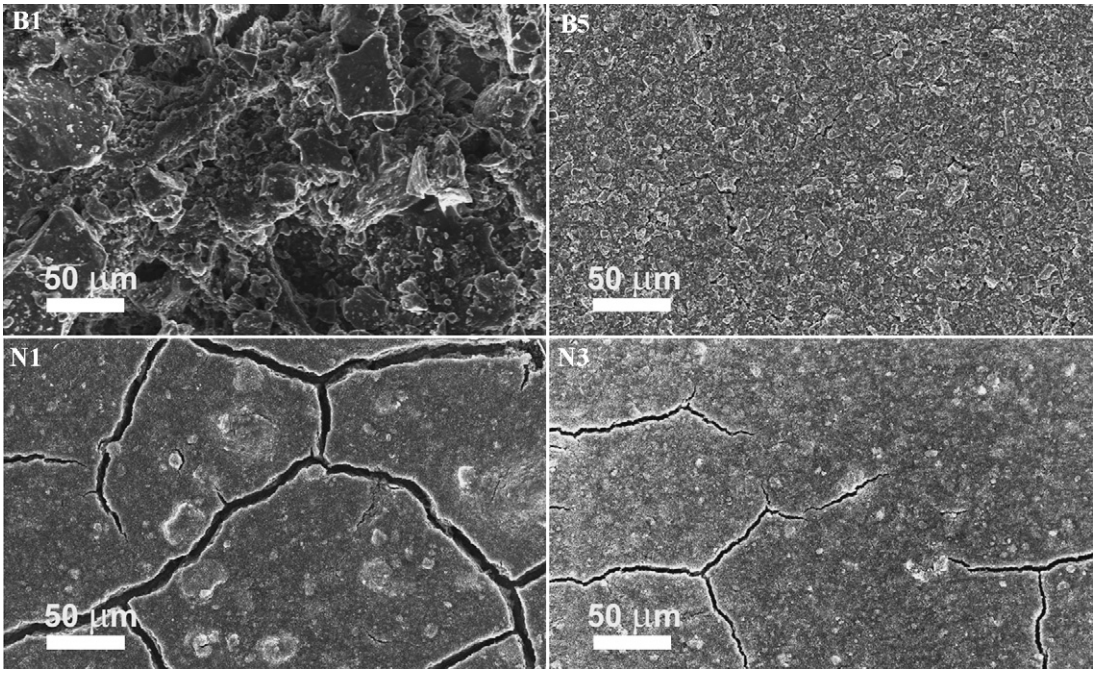

Fig. 5. SEM images of non-cycled coatings used in batteries B1, B5, N1 and N3.

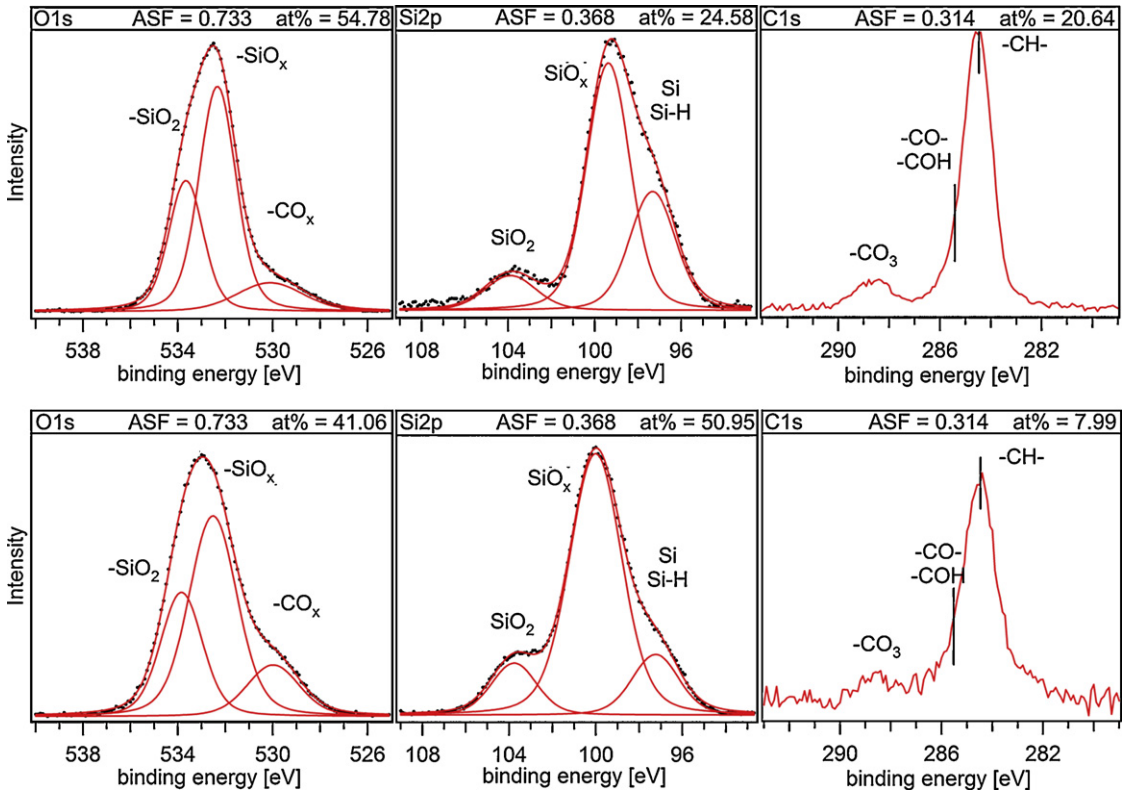

Fig. 6. XP core-level spectra of ethanol-treated (top) and untreated silicon (bottom). For better illustration, the maximum peak intensities have been normalized. The atomic concentration has been derived from the integrated spectral intensity of the respective peak and weighted by atomic sensitivity factors of the spectrometer (ASFs) [12].

between ethanol and Si. Silicon powder usually contains thin native SiO_2 layer on the surface and silanol groups [13]. This type of surface coming in to contact with ethanol can decompose EtOH molecules via breakage of C–H, Et–OH and EtO–H bonds. Ethanol molecules and products can interact with siloxane and silanol bonds in various extends forming new Si–H, SiO–H and Si–OEt bonds in addition to the chemically bonded acetaldehyde, ethylene and other products created during ethanol surface reactions [14]. This type of grafting behaviour on silicon surfaces exposed to alcohols is well known [15–17], though in this work it is applied for the first time to improve Si-anode performance.

4. Conclusions

Preparation of high-silicon content anode films, using EtOH:H_2O as a solvent, increases the capacity of the battery. A possible explanation for this phenomenon is that ethanol, as the more volatile species, evaporates faster initially during the drying process and thus creates more open porosity in the CMC-binder, which in turn provides a better access to a volume of electrode and a larger surface of silicon particles. The effect is more pronounced in the case of nano-Si as it has higher surface area, which may be easier blocked by polymerised CMC than in the case of materials with larger particle-size. In case of bulk-Si this effect is therefore less obvious, and leads only to a slight improvement in the cell capacity, probably also due to opening a larger surface area of active material. However, as the ethanol–water solution in ratio about 30:70 has the highest viscosity [18], improvement of electrode performance can be attributed to more homogeneous carbon black dispersion in electrode, assuring uniform conductive network.

The ethanol treatment of nano-Si has the effect of stabilizing the electrode cycling behaviour. It de-agglomerates nano-Si, but the XPS results also indicate surface functionalisation, which might improve wetability and leads to better cycling performance.

References

[1] U. Kasavajjula, C. Wang, A.J. Appleby, J. Power Sources 163 (2007) 1003–1039.
[2] M. Yoshio, T. Tsumura, N. Dimov, J. Power Sources 146 (2005) 10–14.
[3] B.A. Boukamp, G.C. Lesh, R.A. Huggins, J. Electrochem. Soc. 128 (1981) 725–729.
[4] C.K. Chan, H. Peng, G. Liu, K. McIlwrath, X.F. Zhang, R.A. Huggins, Y. Cui, Nature Nanotech. 3 (2008) 31–35.
[5] J. Graetz, C.C. Ahn, R. Yazami, B. Fultz, Electrochem. Solid-State Lett. 6 (2003) B194–B197.
[6] N. Ding, J. Xu, Y. Yao, G. Wegner, I. Lieberwirth, C. Chen, J. Power Sources 192 (2009) 644–651.
[7] M.K. Datta, P.N. Kumta, J. Power Sources 158 (2006) 557–563.
[8] X. Yang, Z. Wen, X. Xu, B. Lin, S. Huang, J. Power Sources 164 (2007) 880–884.
[9] W. Wang, M.K. Datta, P.N. Kumta, J. Mater. Chem. 17 (2007) 3229–3237.
[10] J. Li, R.B. Lewis, J.R. Dahn, Electrochem. Solid-State Lett. 10 (2007) B17–B20.
[11] V. Bolotov, Y. Sten'kin, V. Roslikov, V. Kang, I. Ponomareva, S. Nesov, Semiconductors 43 (2009) 925–928.
[12] J.F. Moulder, W. Stickle, P. Sobol, K. Bomben, Handbook of X-ray Photoelectron Spectra, PerkinElmer, 1995.
[13] Y. Wang, M. Ferrari, J. Mater. Sci. 35 (2000) 4923–4930.
[14] C.-C. Chang, M.-C. Shu, J. Phys. Chem. B 107 (2003) 7076–7087.
[15] J.T.J. Yates, J.A.J. Glass, E.A. Wovchko, Surf. Sci. 338 (1995) 125–137.
[16] K. Edamoto, Y. Kubota, M. Onchi, M. Nishijima, Surf. Sci. 146 (1984) L533–L539.
[17] M.P.J. Peeters, T.N.M. Bernards, M.J. Van Bommel, J. Sol–Gel Sci. Technol. 13 (1998) 71–74.
[18] M. Yusa, G.P. Mathur, R.A. Stager, J. Chem. Eng. Data 22 (1977) 32–35.